Influence of batch-to-batch material variations on grindability of a medium-carbon steel

Journal of Manufacturing Processes 73 (2022) 463–470

Contents lists available at ScienceDirect

Journal of Manufacturing Processes

journal homepage: www.elsevier.com/locate/manpro

Influence of batch-to-batch material variations on grindability of a medium-carbon steel

Philipp Hoier [a], Bahman Azarhoushang [b], Per Lundin [c,1], Amir Malakizadi [a], Jeffrey Badger [d], Albin Stormvinter [e], Thomas Björk [f], Uta Klement [a], Fukuo Hashimoto [g], Peter Krajnik [a,*]

[a] Department of Industrial and Materials Science, Chalmers University of Technology, Gothenburg, Sweden
[b] Institute of Precision Machining, Furtwangen University of Applied Sciences, Villingen-Schwenningen, Germany
[c] Schlumpf Scandinavia AB, Skarpnäck, Sweden
[d] The Grinding Doc, San Antonio, TX, USA
[e] RISE Research Institutes of Sweden, Gothenburg, Sweden
[f] Ovako AB, Stockholm, Sweden
[g] Advanced Finishing Technology Ltd., Akron, OH, USA

ARTICLE INFO

Keywords:
Grinding
Grindability
Surface integrity

ABSTRACT

This study addresses the influence of material variations on the grindability of crankshaft steel. Most previous studies on the effect of material microstructure on grindability involve comparisons of significantly different steel grades. This study, in contrast, is focused on batch-to-batch grindability variations for one steel grade, a scenario frequently occurring in industry where batches from different steel makers are fed into a production line. For this purpose, a batch made of recycled steel and a batch made of ore-based steel were compared with regards to microstructure and grindability under identical grinding and dressing conditions. Although both batches met the same material specifications, microstructural variations were identified in terms of grain size and micro-constituents (inclusions, carbonitrides). While specific grinding energy, residual stress and full-width at half-maximum profiles of ground surfaces were the same for both batches, the recycled batch showed different and unfavorable variation in wheel wear and Barkhausen noise (BN) response. Larger fractions of oxide inclusions and larger grain sizes (affected by carbonitrides) were present in the recycled batch, which were the likely reasons for the differences in wheel wear and BN response, respectively. These findings may aid grindability improvement by steel-grade adjustments, e.g. modification of the distribution and type of inclusions and/or amount of elements forming carbonitrides. Furthermore, the results highlight the importance of understanding and controlling material microstructure, as existing in-line quality by BN control may not always be able to correctly indicate surface integrity, which could lead to misinterpretations (e.g. false part-rejection on the assumption of grinding burn).

1. Introduction

The manufacture of automotive crankshafts includes a number of material-conversion processes (e.g. forging, soft machining, heat treatment) followed by grinding and superfinishing. Grinding is a crucial finishing step as it provides the required form, dimensional accuracy and surface integrity. While the recent advancement in modelling the geometry and kinematics of crankshaft grinding led to optimized feed increments to reduce cycle time [1], little attention was given to understanding the material effects on the grinding process. The need for a more balanced approach to address both process and material aspects in grinding was already pointed out by Doyle and Dean [2]. The authors established that the information on materials is often incomplete or missing and that production is, to a large extent, unaware of the influence of materials on the grinding process.

This is a common problem for end-users in the automotive industry. In the project associated with the present work, two companies observed firsthand variations between grinding recycled and ore-based (virgin) steel batches, despite all material conforming to the same steel grade specification and the same grinding or dressing parameters. The

* Corresponding author.
E-mail address: peter.krajnik@chalmers.se (P. Krajnik).
[1] Now at Lundin Stress Service AB, Rönninge, Sweden.

https://doi.org/10.1016/j.jmapro.2021.11.012
Received 7 September 2021; Received in revised form 27 October 2021; Accepted 1 November 2021
Available online 23 November 2021

observed variations primarily referred to obtainable dressing intervals. However, the end-users also noted differences with respect to permissible material removal rates and quality-inspection results as indicated by Barkhausen noise non-destructive testing. Such variations pose severe problems in the industry, which wants to avoid adjusting grinding and dressing parameters every time a particular steel batch – obtained from different suppliers – is fed into the production line. To evaluate and better understand these potential differences, batch-to-batch material variations need to be assessed in the context of grindability.

In 1981, König and Messer [3] presented an attempt to address all factors that influence the grinding process, and then described and quantified the grindability of a material. They highlighted the complexity of the system and that the grindability of a material cannot be characterized by one single material characteristic alone. Instead, they mentioned the possibility of combining multiple process characteristics measured during grinding experiments, to form the so-called grindability index.

Following the general definition of machinability, grindability can be considered as the ease at which a material can be ground under given conditions while evaluating the process outputs under defined criteria such as:

- Mechanical: e.g. specific grinding energy (relating to material flow stress, strain, strain rate, hardness, etc.);
- Tribological: friction and wheel wear (caused by grit/bond fracture, microchipping, attrition processes/abrasive dulling, chemical reaction between the workpiece and the abrasive, etc.);
- Thermal: grinding temperature and tendency for thermal damage (workpiece burn by e.g. tempering, formation of tensile residual stresses and/or material phase transformations such as rehardening).

Previous studies of the effects of material microstructure on the grinding process are primarily focused on the differences in grindability between different steel grades. For example, Torrance et al. [4] compared the grindability of a plain-carbon-steel grade to that of an alloy bearing-steel grade and noticed significant differences regarding their susceptibility to grinding burn when grinding under identical conditions. However, they did not report possible material-related reasons for this observation.

Murthy et al. [5], compared the grindability of an austenitic manganese steel grade to that of a micro-alloyed grade as well as a low-alloy steel grade. These steel grades were specifically chosen to test materials at opposite extremes with respect to metallurgical characteristics such as work hardening and phase transformations. In this way it was possible to identify material effects on grindability assessed via grinding forces, specific grinding energy, chip formation and surface integrity.

Similarly, Badger [6] studied metallurgical effects on grindability by assessing wheel wear and power consumption during grinding of eighteen different grades of high-speed steel and concluded that the size of vanadium carbides in the tested grades varied significantly. The size of carbides was the dominant factor affecting grindability in terms of wheel wear and grit dulling.

The above-mentioned investigations focused on the grindability of different steel grades, often in grades with major metallurgical differences. In contrast, the effect on grindability of material variations occurring in the same steel grade has rarely been studied. Recently, Sridharan et al. [7] applied varying heat treatments to a bearing steel grade for the purpose of creating different microstructures (bainitic vs. bainitic-martensitic) and assessed the resulting grindability in terms of specific grinding energy, wheel wear (G-ratio), and part distortion. It was demonstrated that microstructural aspects such as phase composition and carbide fraction significantly affect the grindability. In industrial practice, the austenitizing, quenching and tempering cycles are carefully designed and controlled to obtain a robust heat treatment process – with the aim of reducing microstructural variations prior to grinding. However, in actual production there are still variations in

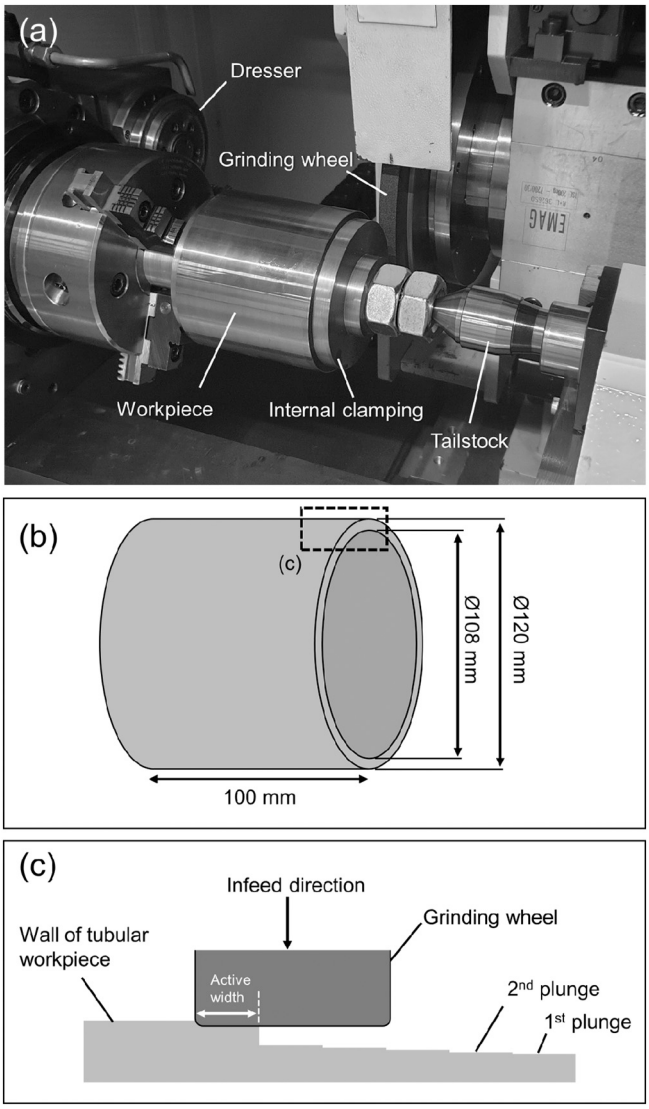

Fig. 1. Experimental setup of grinding tests (a), workpiece geometry (b), and setup during wheel wear tests (c).

times and temperatures, which can result in slight variations in material microstructures.

To the best of our knowledge, this is the first study addressing the effects of supplier-dependent material variations on the grindability of the same steel grade after applying the same heat treatment. Two steel batches undergoing the same heat treatment are in focus: one made of 100% recycled material, and the other being an ore-based batch of the same steel grade. First, the grindability is experimentally assessed by comparing the measured specific grinding energy (mechanical aspect), wheel wear (tribological aspect) and surface integrity (thermal aspect) of both batches. Next, the ground workpieces are analyzed and compared using in-depth material-characterization and material-modelling tools to identify metallurgical differences. Finally, the material differences are correlated with the respective aspects of grindability.

2. Experimental

The experimental setup for the cylindrical-plunge-grinding experiments can be seen in Fig. 1a. The goal was to compare the grindability of two batches of the same medium-carbon steel grade (carbon content specified as 0.41 to 0.46 wt%), heat treated under the same conditions. The chemical composition of the material grade cannot be revealed due

Table 1
Experimental parameters for dressing and cylindrical grinding tests.

Machine tool	EMAG HG 204S
Coolant	Synthetic straight oil
Abrasive wheel type	Vitrified cBN, "B181 C125"
Abrasive wheel diameter [mm]	400
Abrasive wheel width [mm]	15
Grinding wheel speed [m/s]	120
Feed rate [mm/min]	0.61
Workpiece rotation [rpm]	140
Grinding width [mm]	5
Material removal rate [mm^3/s]	19.16
Specific material removal rate [$mm^3/mm \cdot s$]	3.83
Dresser type	Diamond roll
Dressing speed ratio	+0.8
Dressing overlap ratio	3.5
Dressing depth [μm]	5
Dressing passes	>6

to proprietary restrictions. The two steel batches were supplied by different steel producers/companies (recycled vs. ore-based). Vacuum degassing and deoxidization (Al-killed) was applied during steelmaking of both batches. Tubular workpieces (see Fig. 1b) were fabricated from the two solid steel bars and subsequently heat treated (870 °C austenitizing for 1 h, water quenching) and tempered under the same conditions (230 °C for 2 h). The heat treatment yielded a fully martensitic microstructure throughout the tube walls with an average hardness of 574 ± 7.6 HV1 and 582 ± 7.5 HV1 for the recycled and ore-based batches, respectively.

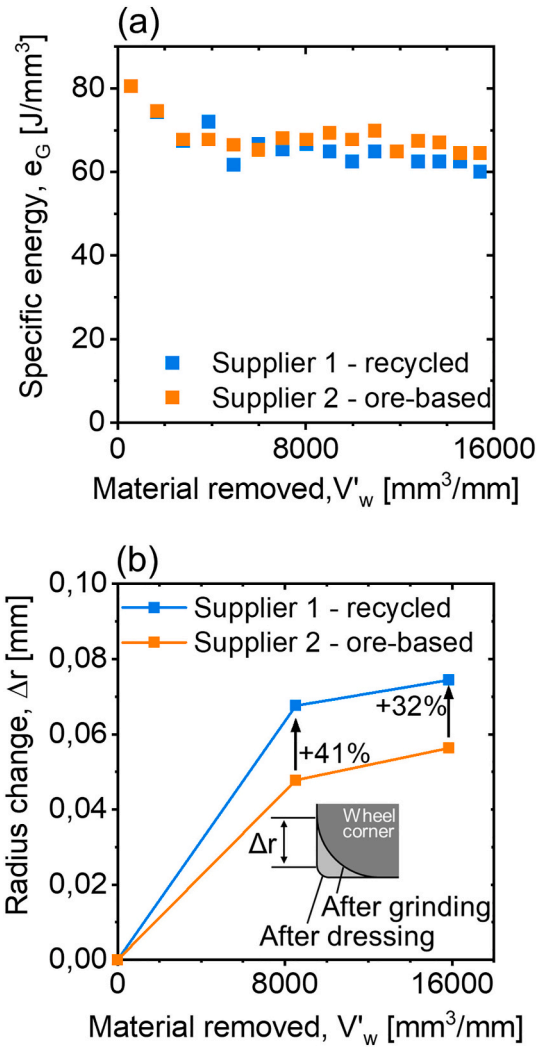

Fig. 2. Specific grinding energy (a) and localized corner wear (b) vs. material removed for the two steel batches.

Two sets of grinding tests were conducted with the goal of comparing the two steel batches with respect to (i) wheel wear and (ii) obtained surface integrity. The spindle power was measured throughout both tests and the corresponding specific grinding energy, e_G (in J/mm^3) was calculated according to:

$$e_G = \frac{P_t - P_0}{Q},$$

where P_t is the total measured spindle power in Watts, P_0 is the idle power in Watts, and Q is the material removal rate in mm^3/s. The material removal rate, Q is defined as:

$$Q = \frac{\pi \cdot f \cdot d_w \cdot b_g}{60},$$

where f is the plunge feed rate in mm/min, d_w is the workpiece diameter in mm, and b_g is the grinding width in mm. During the wheel-wear tests, subsequent cylindrical-grind plunges were offset axially by 5 mm, with a gradual reduction in radial infeed to ensure consistent 5 mm wheel-workpiece contact (Fig. 1c). Wheel wear was quantified periodically by plunging the wheel into an aluminum sheet – after dressing and at specific intervals throughout the tests, followed by measuring the respective sheets using a tactile profilometer.

The second set was focused on determining if there were inherent differences in grit-contact mechanisms and forces (i.e., plowing and chip-formation energies) between the two batches. It was designed to exclude the potential effects of any differences in transient wheel wear – namely, the rate of grit-dulling (and therefore power, heat generation and, consequently, workpiece temperature) – between the materials. The wheel was dressed only at the beginning of the trials, followed by multiple plunges while switching back-and-forth between the two steel batches. In this way, the grinding process could be assessed independent of the workpiece material's effect on wheel sharpness (i.e., both materials would be ground with the same wheel sharpness), enabling the resulting surface integrity to be assessed for consistent grinding heat input.

The grinding tests used a vitrified-bonded cubic-boron-nitride (cBN) wheel (B181 FEPA grain size, 400 mm wheel diameter, 15 mm wheel width). A diamond form roller was used to dress the grinding wheel with a dressing speed ratio of +0.8, an overlap ratio of 3.5, and a dressing depth of 5 μm. At least six dressing passes (total dressing depth of at least 30 μm) were made prior to each test to re-establish the initial grinding wheel topography. Before each wheel wear test in particular, a higher number of 18 dressing passes (90 μm total dressing depth) were performed. Grinding parameters were kept constant for all tests: wheel speed = 120 m/s, infeed rate = 0.61 mm/min, grinding width = 5 mm, workpiece rotational speed = 140 RPM. The specific material removal rate Q'_w (in mm^3/mm · s), i.e. the material removal rate per mm grinding wheel width was calculated by dividing the material removal rate by the grinding width. In the present case this yields $Q'_w = 3.83$ mm^3/mm · s. The total grinding allowance for a single plunge was 3 mm off radius. A synthetic (mineral-oil-free) straight grinding oil was used (Berucut XC 1110, viscosity 9.5–11.6 mm^2/s). A summary of the experimental condition is given in Table 1.

Microscopic changes to the wheel topography were assessed on replicas that reproduced the surface of the grinding wheel, taken after the wheel wear tests. To remove oil, the wheel surface was thoroughly cleaned using acetone. Next, a silicone-based putty was applied to 50-mm-long sections of the grinding wheel to create negative imprints of the surface. An epoxy resin (DIEMET-E) was subsequently cast into the negative imprint. After hardening for 24 h, the resulting positive cast was utilized for detailed analysis in a scanning electron microscope (SEM).

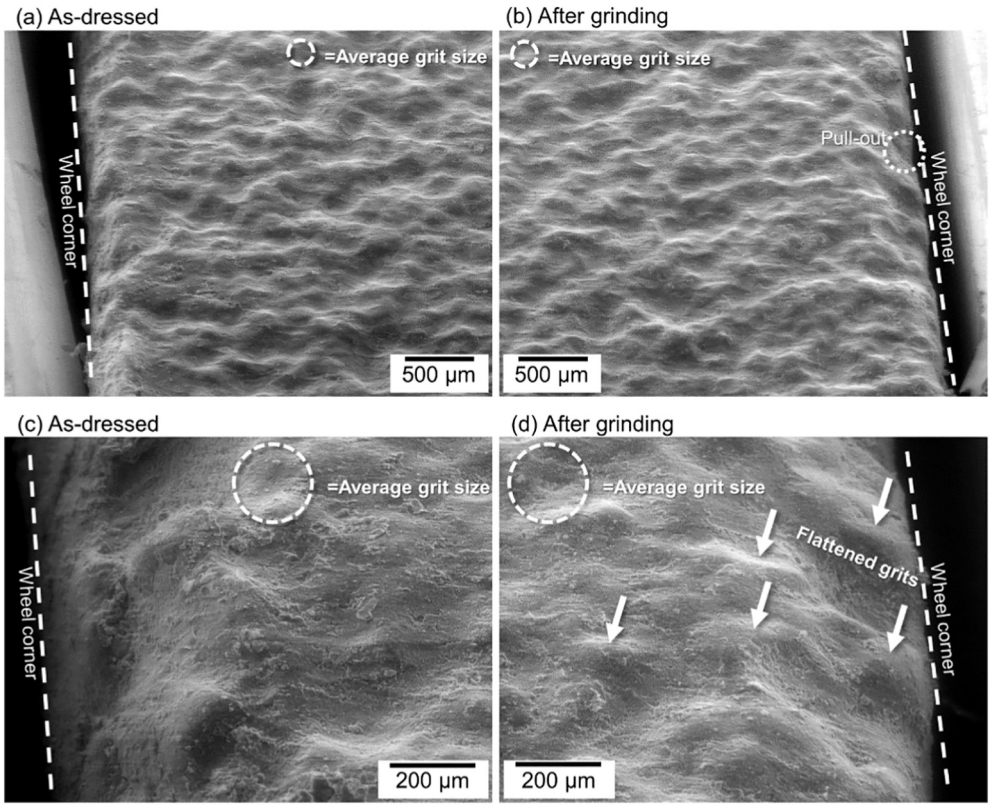

Fig. 3. SEM micrographs showing replicas of the grinding wheel topography directly after dressing (a, c) and after grinding the investigated steel grade (b, d). Flattened protrusions (see arrows in (d)) suggest grit wear by attrition close to wheel corner.

Surface integrity characterization was done by Barkhausen noise (BN) measurements using a Rollscan R300 BN-signal analyzer (sine magnetization wave form, 6 V magnetization voltage, 125 Hz frequency, measurements in the circumferential/grinding direction). A wide-band sensor was used to analyze the signal in the frequency range of 70–200 kHz. Four measurements were made (equally distributed 90° around the circumference of each ground surface) and averaged. Residual stresses and full-width-at-half-maximum (FWHM) values of the associated diffraction data were measured using an XSTRESS 3000 G2R diffractometer with a CrKα X-ray source (30 kV, 9 mA). Six $\sin^2(\chi)$ tilts from −30° to +30° and the lattice deformations for the {211}α–Fe peak were used for determining the stress values. The Young's modulus and Poisson's ratio (used for calculating the stresses) were 211 MPa and 0.3, respectively. The sample surfaces were irradiated through a circular collimator of 1.5 mm diameter, and stepwise electrochemical etching with a solution of NaCl was used to obtain stress depth profiles.

Metallographic comparison of the microstructures of the two steel batches was done on samples extracted from the heat-treated workpieces. The samples were compared against their average Vickers hardness (1 kgf load), their martensite morphology (Nital etch), prior austenite grain size (etched with saturated picric acid, determination of mean lineal intercept length), and non-metallic inclusions (non-etched samples). Light optical microscopy and an SEM equipped with a detector for energy-dispersive X-ray spectroscopy (EDS) were used for imaging the samples and for determining the composition of non-metallic inclusions. The amount and size of different types of non-metallic inclusions in each steel batch were analyzed on 50 backscatter electron detector images (250× magnification) by using *Z*-contrast arising from different mean atomic numbers of non-metallic inclusions compared with the steel matrix. The total investigated area for each workpiece batch was 46 mm^2. Detailed chemical compositions of the test batches were determined by a combination of X-ray fluorescence spectroscopy, combustion analysis and optical emission spectrometry. The batch-specific compositions were then used as input for simulation of the stability of carbonitrides using the thermodynamic simulation tool Thermo-Calc, with TCFE Steels/Fe-alloys database version 9.0 [8].

3. Results and discussion

Results of the specific-energy and wheel-wear tests are summarized in Fig. 2. Both batches exhibited an initial decrease in specific energy with increasing material removed (about 15% in three plunges), likely due to typical grit self-sharpening seen with cBN wheels after dressing. For the remaining plunges, the specific grinding energy remained nearly constant at about 65 J/mm^3, with the differences between the batches being below 7%. No step in the wheel was observed at the transition between the active wheel surface and the portion of the wheel that was not in contact with the workpiece during grinding. However, wheel wear at the corner was not insignificant, as shown in Fig. 2b. Here, a larger change in the radius Δr was observed when grinding the recycled steel, even though the total wear was less than half the grit diameter. This situation (of measurable corner wear, but negligible outer-diameter wear) is analogous to production grinding of crankpins, where the grinding aggressiveness (and hence wheel wear) surges in a localized, narrow portion on the radius of the wheel [1]. The appearance of an unfavorable step and/or grinding burn localized on the radius of a crankshaft pin, both caused by irregular wheel wear was observed previously by Oliveira et al. [9], which is consistent with the experience of practicing engineers in industry. Localization of wear at the wheel corner may be further pronounced by the fact that retention of cBN grits located at the very corner is lower as compared with grits on the rest of the wheel.

To gain further insight into the wear phenomenon, a microscopic analysis was made of replicas of the wheel (Fig. 3). The micrographs indicate that a significant portion of corner wear took place in the form of dulling of cBN grits by attritious wear (see arrows in Fig. 3d), with

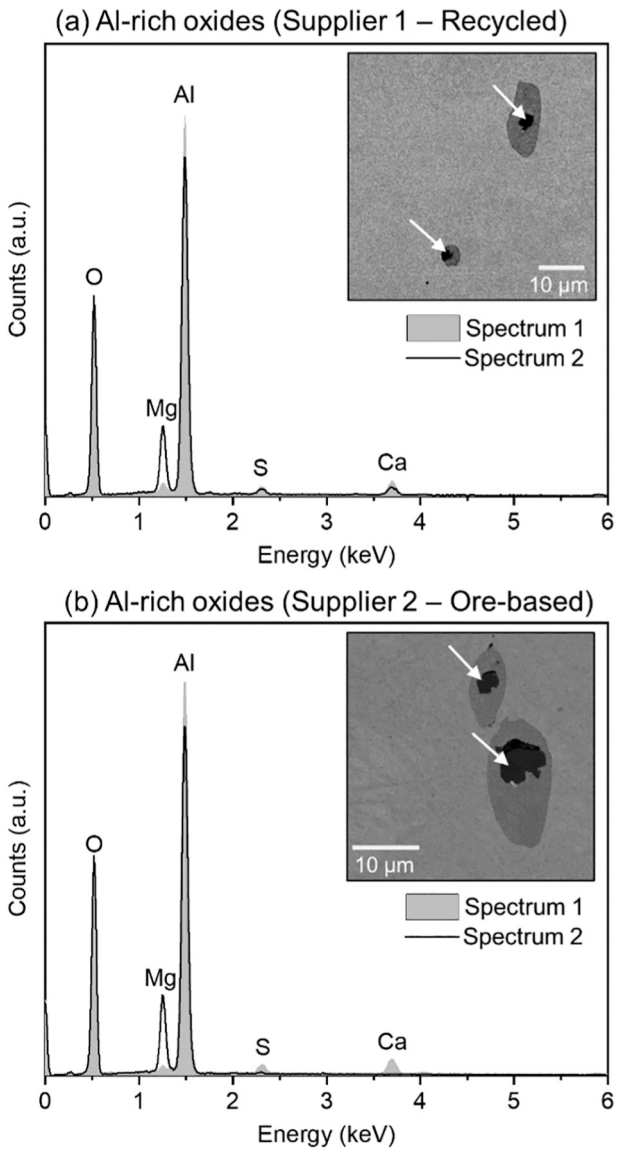

Fig. 4. Examples of EDS spectra showing the composition of oxide inclusions present in (a) the recycled batch, and (b) the ore-based batch. Inserts show SEM micrographs with arrows indicating respective oxide inclusions.

signs of cBN grit pull-out (see Fig. 3b). Attritious wear has previously been reported as an important wear mechanism in grinding of high-speed steel containing significant fractions of hard, abrasive carbides [6]. This wear was accompanied by an increase in grinding power (or specific grinding energy) due to increased rubbing from the dull grits. However, as seen in Fig. 2a, this effect was not observed in the present study. The absence of an increase in specific grinding energy is likely because the significant grit dulling was localized at the very corner of the grinding wheel (see Fig. 3b and d), while the majority of the grinding wheel surface was not subjected to attritious wear. Limited attritious wear on the majority of the active grinding wheel surface is also supported by the absence of a measurable step at the transition toward the inactive portion of the grinding wheel.

Sridharan et al. [7] observed a more pronounced difference in wheel wear (measured as G-ratio) when grinding bearing steel workpieces with an aluminum-oxide wheel. The authors observed a 50% difference in G-ratio for the two distinct bainitic microstructures. They attributed this primarily to the differences in the fractions of hard carbides in the tested workpieces. For the heat-treated workpieces investigated here, hard particles were primarily oxide inclusions. No traces of carbides could be

Table 2
Quantities of non-metallic inclusions in investigated workpieces.

	Sulfides (MnS)		Al-rich oxides (Al_2O_3)	
	Area fraction (%)	Avg. area (μm^2)	Area fraction (%)	Avg. area (μm^2)
Supplier 1—recycled	0.21	35.60	0.0097	9.64
Supplier 2—ore-based	0.17	39.66	0.0051	8.50

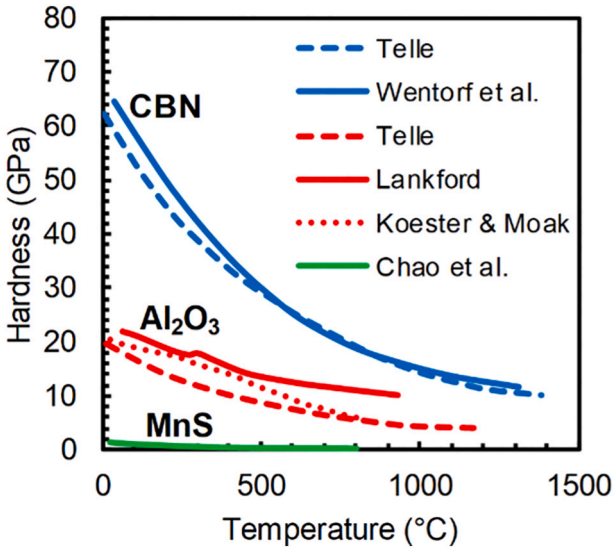

Fig. 5. Reported hardness of cBN, pure Al_2O_3, and MnS. Figure drawn from data reported in [14–18].

observed during the SEM-based examination. The reason for this is likely that the temperature and holding time during tempering of the fully martensitic material only yielded minor precipitation, resulting in very fine carbides such as Fe_3C and/or ε-carbides in the nm-range [10], which were not possible to resolve during the SEM examination.

To see whether differences in inclusions between both material batches played a role in wheel-wear, a detailed microstructural examination was conducted on both materials. Metallographic comparison of the two workpieces revealed that both batches contained sulfide inclusions (MnS) as well as Al-rich oxides, likely Al_2O_3. For both batches, EDS examination was conducted on at least 30 oxides and showed that there are no significant differences regarding their composition when comparing the steel batches with each other. For both batches, all examined oxides were rich in Al with varying trace amounts of Mg and/or Ca and S. Examples of EDS spectra with the described characteristics are provided in Fig. 4. Note that, similar to the oxide inclusions, the composition of MnS inclusions did not vary between both batches.

While showing insignificant differences in terms of composition, the fractions of the identified inclusion types varied between both batches. The amounts of hard oxide inclusions (Al_2O_3) and to a lesser extent the amount of soft sulfide inclusions (MnS) were higher in the recycled batch than in the ore-based batch (see Table 2). The measured area fraction of oxide inclusions in particular was almost double for the recycled batch.

Compared to grinding, the role of workpiece material microstructure on wear has been studied much more systematically in metal cutting, where in-depth material characterization has been extended to also include worn surfaces of the tool, i.e. cutting inserts [11]. An important factor determining the potential of attritious abrasive wear is the hardness ratio between the tool material (here the cBN grit) and the workpiece particle (here the inclusion)—the smaller the hardness ratio

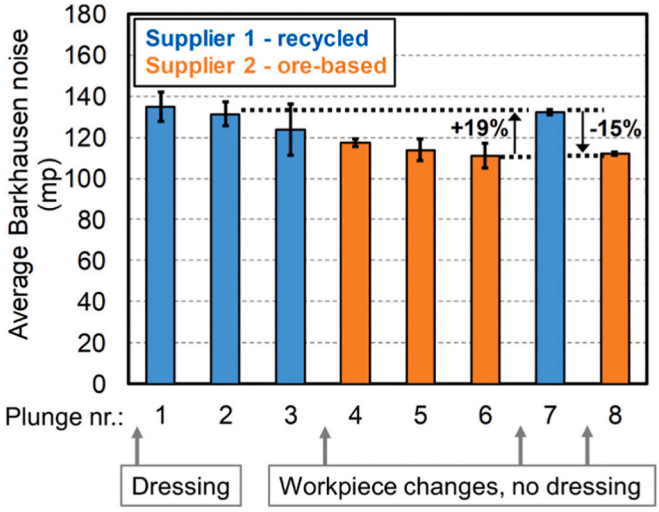

Fig. 6. Barkhausen noise of ground surfaces. Each plunge corresponds to ~1000 mm^3/mm of material removed.

the higher the rate of tool wear. Rabinowicz [12] showed that the rate of tool wear (here cBN) increases rapidly at ratios smaller than 0.8. However, wear by abrasion still occurs for hardness ratios above 1.0, although at much lower rates. Fig. 5 shows that the sulfide inclusions have significantly lower hardness than the cBN grits. In contrast, the Al_2O_3 inclusions have a hardness of approximately half that of cBN at typical grinding temperatures [1]. Here we are encroaching on the ratio where abrasive wear would not be negligible. Badger [6] found that (W, Mo)$_6$C particles produced a non-negligible amount of wear on Al_2O_3 grits – with similar hardness ratios to those found here. This indicates that the greater amount of Al_2O_3 inclusions (and larger size) in the recycled material may be a contributor to the greater cBN wheel wear seen in the tests. In addition, abrasion and attritious wear in brittle materials like cBN are strongly related to their fracture toughness [13], producing grit micro-cracking, which may have also contributed to the greater wheel wear seen for the recycled batch.

Results of BN measurements are presented in Fig. 6. The BN signal depends on the effects that residual stress, hardness and microstructure have on the movement of magnetic domain walls during magnetization of ferromagnetic materials [19]. In the production of crankshafts, BN is used for in-line quality control, with any outlier – i.e. a BN measurement above the control limit – indicating thermal damage and an associated shift toward tensile residual stresses and/or lower hardness. Non-destructive testing solely based on the BN results presented in Fig. 6 would therefore suggest more tensile stresses and/or material softening (i.e. inferior surface integrity) for the recycled material, both usually caused by higher grinding temperatures.

However, this stands in stark contrasts to the similar (or even slightly lower) specific energies measured in the recycled batch (Fig. 2). In addition, the back-and-forth (batch switching) tests – designed to grind both materials while excluding the effect of changing wheel topography – showed no change in specific grinding energy between batches, whereas the changes in material from plunge 6 to plunge 7 to plunge 8 (Fig. 6) yielded changes in the BN response (with the gradual decrease after dressing caused by grit sharpening, independent of material, which is consistent with Fig. 2).

In other words, while the specific energy (and heat input to the workpiece) was expected to be similar for both batches, the BN response was not – and increased when switching from ore-based to recycled (plunges 6 to 7) and then decreased again when switching back to ore-based (plunges 7 to 8). This indicates that there is a difference in the fundamental, material-related BN response between the two batches – independent of the grinding process.

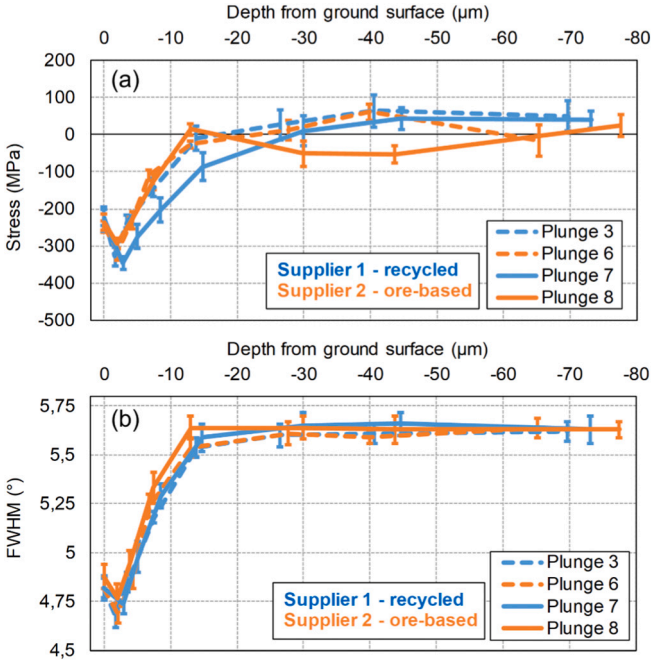

Fig. 7. Depth profiles of (a) residual stresses and (b) FWHM values.

To further investigate the surface integrity of the ground surfaces, residual stress measurements were conducted (Fig. 7). The results are generally confirming that the observed BN differences between the batches are not process related – e.g. caused by different temperatures when grinding the two batches. As seen in Fig. 7, all residual stress measurements show compressive surface stresses (with maximum stress occurring a few µm below the surface), followed by decreasing compressive stress until reaching the near-stress-free bulk material. Hence, almost all stress profiles appear very similar, with only plunge 7 (recycled material) showing slightly more negative (compressive) stresses, which also reach deeper into the material (30 µm), as compared to the other measurements (12 to 20 µm). Higher compressive stresses should however lead to decreased BN intensity, which is the opposite of what has been measured in Fig. 6.

In other words, the higher BN levels for the recycled steel cannot be explained by the differences in residual stresses after grinding. Similarly, the comparison of full-width-half-maximum (FWHM) values, shown in Fig. 7b, reveal very similar profiles for all measurements. FWHM give indications of the surface hardness of the ground material. The results in Fig. 7b indirectly indicate that there are no significant differences in surface hardness of the ground steel batches.

In addition to the stress state and hardness, BN intensity is also influenced by the material's microstructure. While the general martensite structure (see Fig. 8a) and bulk hardness are similar for both materials, significant differences in the measured average size of prior austenite grains can be seen in Fig. 8b. This grain-size difference contributes to the variations in the measured BN signals. The exact influence of grain size on BN response has been subject to numerous studies on different materials with various types of microstructures. As a consequence, conflicting correlations have been reported, which include increasing BN for larger grain size in decarburized steel and for smaller grains in nickel [20].

For steels in the ferritic-pearlitic state, the same trend of increasing BN for larger grains has been reported by Titto et al. [21]. In another study concerning ferritic-pearlitic steel by Ktena et al. [22], the opposite trend has been reported, with larger grains leading to an decrease in BN. Most relevant for the present case is a recent study on induction-hardened camshaft lobes by Tam et al. [23], who found that larger prior austenite grain size leads to higher BN intensities. With respect to

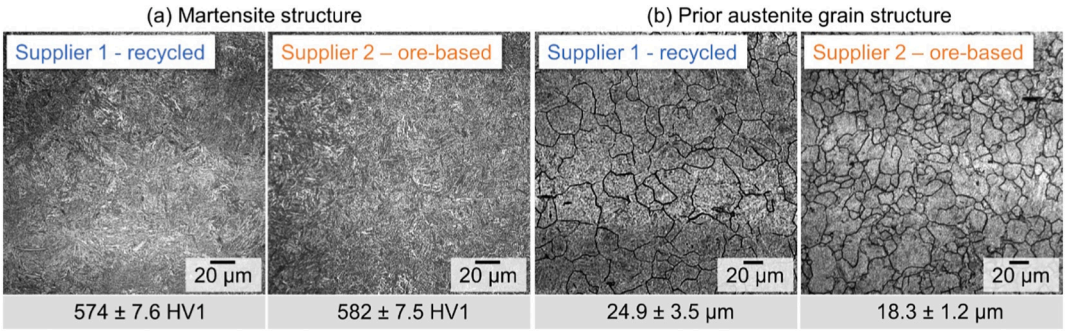

Fig. 8. Material microstructures: (a) martensitic microstructures with average hardness; (b) prior austenite grain structure with average grain size measures (mean lineal intercept length).

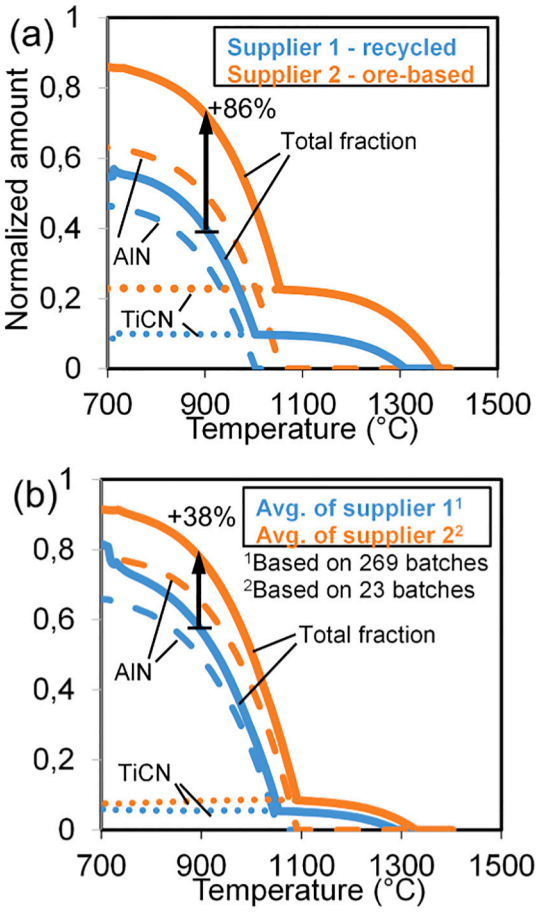

Fig. 9. Simulated amounts of carbonitrides as function of temperature based on (a) composition of the two tested steel batches and (b) average compositions of multiple steel batches of the respective suppliers. Relative differences (in %) in total amount at 900 °C are indicated.

the present case, their finding would suggest that it is the larger grains in the recycled batch that are the reason for the higher level of BN.

In order to understand why the grain size was larger in the recycled batch, the heat-treatment process and grain-growth behavior have to be considered. The possible underlying reasons for the variations in grain size are austenitizing temperature, holding time, and kinetics of grain growth. Considering that the workpieces were all hardened under identical temperature and holding time, it is assumed that different grain-growth kinetics during austenitizing played a key role. Varying amounts of micro-alloying elements can affect the grain-growth behavior during austenitizing by precipitation of very fine, sub-micron-sized carbonitride particles [24].

Considering this, the stability of carbonitrides was investigated using Thermo-Calc Software, with TCFE Steels/Fe-alloys database version 9.0. Fig. 9a shows that in the two tested batches, the sum of stable carbonitrides is higher in the ore-based steel. Higher amounts of such particles in the appropriate size range limits austenite grain growth by pinning grain boundaries during austenitizing [25]. This may explain the smaller grain size of the ore-based steel batch. The plots in Fig. 9b are based on average steel compositions of the two concerned suppliers and demonstrate the same trend observed in this work. On average, the ore-based steel from supplier 2 contains larger fractions of grain growth-inhibiting carbonitrides during hardening as compared to the recycled steel of supplier 1.

To summarize, the apparent grindability differences reported by some automotive OEMs (see section 1) could be confirmed only regarding wheel wear behavior. Higher wheel wear associated with grinding the recycled steel batch might be linked to higher amounts of oxide inclusions in the tested workpieces. However, no batch-dependent process variations regarding heat generation (suggested by similar specific grinding energy) and resulting surface integrity (suggested by similar residual stress and FWHM profiles) were identified when grinding both batches under similar grinding conditions. However, it was discovered that when assessing surface integrity only by BN analysis, as the case in an industrial scenario, microstructural variations due to different grain size for different batches can lead to misinterpretations when assessing ground surface integrity. Microstructural variations, such as grain size differences caused by varying amounts of carbonitride-forming elements, might have contributed to the perceived surface integrity differences between recycled and ore-based steel batches reported by the automotive OEMs.

It should be noted that in scenarios where more material is removed (extending beyond the lab experiments conducted here), the grit dulling/flattening at the wheel corner observed here could extend into larger portions of the wheel width [9]. In this case, the larger amount of rubbing would likely increase the specific grinding energy and, consequently, heat input and workpiece temperature, leading to deteriorating surface integrity. Based on the wheel-wear results, it is expected that this scenario may arise earlier for the tested recycled batch as compared with the ore-based batch. This may have further contributed to the perception of inferior grindability of recycled material batches.

The identified material variations in this work regarding micro-alloying elements and non-metallic inclusions are not likely to be a direct result of the recycling process, i.e. can occur irrespective of whether the steel is recycled or ore-based. Instead, they are steel-supplier specific, caused e.g. by slightly varying practices in the steel-making process.

4. Conclusions

An investigation was made into the grindability of recycled and ore-

based batches of the same crankshaft-steel grade and with the same heat treatment. Despite meeting the same material specifications, variations were observed in the microstructure with regards to micro-constituents (inclusions, carbonitrides) and grain size. While specific grinding energy, resulting residual stress and FWHM profiles of ground surfaces were unaffected, wheel wear and BN response were both higher in the recycled batch.

Higher wheel wear by attrition during grinding the recycled batch was linked to a higher fraction of oxide inclusions in the workpiece. Unfavorable BN results for the recycled batch (despite similar residual stress and FWHM profiles as the ore-based batch) were caused by larger grains originating from differences in carbonitride-forming elements which affected the grain growth behavior during heat treatment.

The results of this study may aid grindability improvement by steel-grade adjustments, e.g. by modifying the distribution and type of inclusions and/or micro-alloying elements forming carbonitrides. In addition, the findings stress the importance of understanding and controlling material microstructure, as existing in-line quality control may not always be able to correctly indicate surface integrity, which could lead to misinterpretations (e.g. false part-rejection on the assumption of grinding burn).

Declaration of competing interest

Peter Krajnik reports financial support was provided by Sweden's Innovation Agency.

Acknowledgments

The authors thank Robert Bösinger for dedicated experimental work and Nastja Mačerol and Fredrik de Geer for valuable discussions. Members of the International Grinding Centre (IGC) belonging to Chalmers Centre for Metal Cutting Research (MCR) are acknowledged. This work has been performed with the financial support from Sweden's Innovation Agency (CRANK-STEEL project; grant no. 2017-02908).

References

[1] Dražumerič R, Roininen R, Badger J, Krajnik P. Temperature-based method for determination of feed increments in crankshaft grinding. J Mater Process Technol 2018;259:228–34. https://doi.org/10.1016/j.jmatprotec.2018.04.032.
[2] Doyle ED, Dean SK. Insight into grinding from a materials viewpoint. CIRP Ann Manuf Technol 1980;29:571–5. https://doi.org/10.1016/s0007-8506(16)30155-x.
[3] König W, Messer J. Influence of the composition and structure of steels on grinding process. CIRP Ann Manuf Technol 1981;30:547–52. https://doi.org/10.1016/S0007-8506(07)60165-6.
[4] Torrance AA, Stokes RJ, Howes TD. Steel composition effects on grindability and rolling contact fatigue resistance of bearing steels. J Tribol 1985;107:496–500. https://doi.org/10.1115/1.3261115.
[5] Murthy JKN, Chattopadhyay AB, Chakrabarti AK. Studies on the grindability of some alloy steels. J Mater Process Technol 2000;104:59–66. https://doi.org/10.1016/S0924-0136(00)00516-1.
[6] Badger J. Grindability of conventionally produced and powder-metallurgy high-speed steel. CIRP Ann Manuf Technol 2007;56:353–6. https://doi.org/10.1016/j.cirp.2007.05.081.
[7] Sridharan U, Peurifoy J, Bedekar V. Influence of material microstructure on grindability of bearing steel. CIRP Ann Manuf Technol 2021;00:10–3. https://doi.org/10.1016/j.cirp.2021.04.009.
[8] Andersson JO, Helander T, Höglund L, Shi P, Sundman B. Thermo-Calc & DICTRA, computational tools for materials science. Calphad 2002. https://doi.org/10.1016/S0364-5916(02)00037-8.
[9] Oliveira JFG, Silva EJ, Gomes JJF, Klocke F, Friedrich D. Analysis of grinding strategies applied to crankshaft manufacturing. CIRP Ann Manuf Technol 2005;54:269–72. https://doi.org/10.1016/S0007-8506(07)60100-0.
[10] Speich GR, Leslie WC. Tempering of steel. Metallurgical Transaction 1972;3:1043–54.
[11] Hoier P, Malakizadi A, Klement U, Krajnik P. Characterization of abrasion- and dissolution-induced tool wear in machining. Wear 2019;426–427:1548–62. https://doi.org/10.1016/j.wear.2018.12.015.
[12] Rabinowicz E. Abrasive wear resistance as a materials test. Lubr Eng 1977;33:378–81.
[13] Zum Gahr KH. Wear by hard particles. Tribol Int 1998;31:587–96. https://doi.org/10.1016/S0301-679X(98)00079-6.
[14] Telle R. Properties of ceramics. In: Handb ceram grind polishing; 1999. p. 1–64. https://doi.org/10.1016/b978-081551424-4.50003-2.
[15] Wentorf RH, DeVries RC, Bundy FP. Sintered superhard materials. Science (80-) 1980;208:873–80. https://doi.org/10.1126/science.208.4446.873.
[16] Lankford J. Comparative study of the temperature dependence of hardness and compressive strength in ceramics. J Mater Sci 1983;18:1666–74. https://doi.org/10.1007/BF00542061.
[17] Koester R, Moak D. Hot hardness of selected borides, oxides, and carbides to 19OO °C. J Am Ceram Soc 1967;50:290–6.
[18] Chao HC, Van Vlack LH, Oberlin F, Thomassen L. Inclusion deformation: II. Hardness of MnS-FeS microstructures. In: Univ Michigan, tech reports; 1962.
[19] Jawahir IS, Brinksmeier E, M'Saoubi R, Aspinwall DK, Outeiro JC, Meyer D, et al. Surface integrity in material removal processes: recent advances. CIRP Ann Manuf Technol 2011;60:603–26. https://doi.org/10.1016/j.cirp.2011.05.002.
[20] Ranjan R, Jiles DC, Buck O, Thompson RB. Grain size measurement using magnetic and acoustic Barkhausen noise. J Appl Phys 1987;61:3199–201. https://doi.org/10.1063/1.338900.
[21] Titto S, Otala M, Säynäjäkangas S. Non-destructive magnetic measurement of steel grain size. Non-Destr Test 1976;9:117–20. https://doi.org/10.1016/0029-1021(76)90239-5.
[22] Ktena A, Hristoforou E, Gerhardt GJL, Missell FP, Landgraf FJG, Rodrigues DL, et al. Barkhausen noise as a microstructure characterization tool. Phys B Condens Matter 2014;435:109–12. https://doi.org/10.1016/j.physb.2013.09.027.
[23] Tam PL, Hammersberg P, Persson G, Olavison J. Case depth evaluation of induction-hardened camshaft by using magnetic Barkhausen noise (MBN) method. Nondestruct Test Eval 2020:1–21. https://doi.org/10.1080/10589759.2020.1813284.
[24] Baker TN. Microalloyed steels. Ironmak Steelmak 2016;43:264–307. https://doi.org/10.1179/1743281215Y.0000000063.
[25] Adrian H, Pickering FB. Effect of titanium additions on austenite grain growth kinetics of medium carbon V–Nb steels containing 0.008–0.018%N. Mater Sci Technol 1991;7:176–82. https://doi.org/10.1179/026708391790194860.